Photospheres, Comptonization and X-ray Lines in Gamma-Ray Bursts

P. Mészáros [1,2,3]

[1] *Pennsylvania State University, 525 Davey, University Park, PA 16802*
[2] *California Institute of Technology, MS 105-24, Pasadena, CA 91125*
[3] *E-mail address: nnp@astro.psu.edu*

Abstract. Steep X-ray spectral slopes, X-ray excesses and preferred spectral energy breaks in the 0.1–0.3 MeV range are discussed as the possible consequences of the photospheric component of the GRB relativistic outflow, and of pair breakdown in internal shocks leading to Comptonization on semi-relativistic electrons or MHD waves. We also discuss the X-ray and UV spectra of GRB afterglows occurring in a dense environment characteristic of massive stellar progenitors, including their ability to produce detectable Fe or other metallic line features.

PHOTOSPHERES, SHOCKS AND PAIRS

A significant fraction of bursts appear to have low-energy spectral slopes steeper than 1/3 in energy [1,2]. This has motivated consideration of a thermal or nonthermal [3,4] Comptonization mechanism, while leaving the astrophysical model largely unspecified. There is also evidence that the apparent clustering of the break energy of GRB spectra in the 50–500 keV range may not be due to observational selection [1,5,6]. Models using Compton attenuation [7] require reprocessing by an external medium whose column density adjusts itself to a few g cm^{-2}. More recently, a preferred break has been attributed to a blackbody peak at the comoving pair recombination temperature in the fireball photosphere [8]. In order for such photospheres to occur at the pair recombination temperature in the accelerating regime requires an extremely low baryon load. For very large baryon loads, a different explanation has been invoked [9] involving scattering of photospheric photons off MHD waves in the photosphere, which upscatters the adiabatically cooled photons up to the observed break energy.

Motivated by the above observations, these ideas have been synthesized [10] to produce a generic scenario in which the presence of a photospheric component as well as shocks subject to pair breakdown can produce steep low-energy spectra and

CP526, *Gamma-Ray Bursts: 5th Huntsville Symposium,* edited by R. M. Kippen, et al.

preferred breaks (see Figure 1). In some of our previous work [11,12] considering photospheres and pair formation, their thermal character, the uncompensated photosphere redshift in the coasting phase, and the requirement of a power law extending to GeV energies were arguments in favor of a synchrotron and inverse Compton mechanism in shocks. The latter should, indeed, play a significant role in any model. However, a photosphere is always present, even if not always dominant. If the photosphere occurs in the accelerating regime where $\Gamma \propto r$, its energy is comparable to that of shocks which may occur further out, and the energy at which the black-body peak (T) is observed is in the "magic" range near 0.5 MeV, for $\eta \geq \eta_*$, where $\eta = L/\dot{M}c^2 \rightarrow \Gamma_f$ is the terminal bulk Lorentz factor and $\eta_* = (L\sigma_T/4\pi m_p c^3 r_o)^{1/4} \simeq 10^3(L_{52}r_7^{-1})^{1/4}$. Both its peak energy and its total energy are lower if the photosphere occurs in the coasting phase ($\eta \leq \eta_*$). A steep low-energy spectral slope is provided by the Rayleigh-Jeans part of the photosphere, and a low-energy excess or terrace by its Wien part. A high-energy power law extending above this up to GeV requires, however, a separate explanation. One possibility is up-scattering of photospheric photons in the $\tau_T \gtrsim 1$ region by Alfvén waves, whose energy may be a fraction of the bulk kinetic energy [9]. This leads to a Comptonized broken power law spectrum (PHC) in xF_x ($x = h\nu/m_e c^2$) of slope 1 up to the "magic" break energy $x \lesssim 1$, and slope 0 up to $x \lesssim \eta$ above that (Fig. 1). The energy in this PHC wave-Comptonized component can be substantial relative to the photosphere, and equals the ratio of wave to bulk kinetic energy.

Above the photosphere, internal shocks are expected to occur [12], which would lead to a nonthermal Synchrotron/IC spectrum (S) in addition to the above. How-

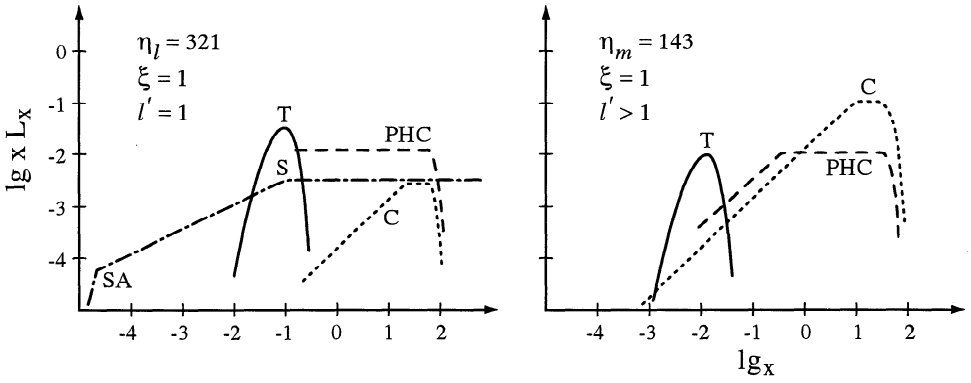

FIGURE 1. Luminosity per decade xL_x vs. $x = h\nu/m_e c^2$ for two values of $\eta = L/\dot{M}c^2$ and marginal (left) or large (right) pair compactness. T: thermal photosphere, PHC: photospheric Comptonized component; S: shock synchrotron; C: shock pair dominated Comptonized component [10]

ever, if the compactness parameter ℓ' (or comoving luminosity) is high, pair formation occurs which could produce a self-regulated low pair (comoving) temperature $\Theta'_p = kT'/m_e c^2 \sim 10^{-1}$ favoring Comptonization [13]. In this $\ell' \geq 1$ case, thermal Comptonization on the sub-relativistic electrons leads to another Comptonized component (C) of slope 1 up to an observer-frame energy $x \sim \Theta'_p \eta \sim 10^{-1}\eta$. Above this, if scattering off waves also occurs in the shocks, a second component of slope 0 would extend above it to $x \lesssim \eta$.

X-RAY AND UV LINE SPECTRA OF GRB

The environment in which a GRB occurs may also lead, in the afterglow phase, to specific spectral signatures from the external medium imprinted in the continuum, such as atomic edges and lines [14–16]. These may be used both to diagnose the chemical abundances and the ionization state (or local separation from the burst), as well as serving as potential alternative redshift indicators. (In addition, the outflowing ejecta itself may also contribute blue-shifted edge and line features, especially if metal-rich blobs or filaments are entrained in the flow from the disrupted progenitor debris [17], which could serve as diagnostic for the progenitor composition and outflow Lorentz factor). An interesting prediction [16] is that an Fe K-α X-ray *emission* line could be a diagnostic of a hypernova, since in this case one may expect a massive envelope at a radius comparable to a light-day where $\tau_T \lesssim 1$, capable of reprocessing the X-ray continuum by recombination and fluorescence (see also [18,19]). Detailed radiative transfer calculations have been performed to simulate the time-dependent X/UV line spectra of massive progenitor (hypernova) remnants [20], see Figure 2. Two types of hypernova environment geometries were considered, which are illuminated by a typical time-dependent broken power law afterglow continuum spectrum. One model consists of a dense shell, such as a supernova remnant, which could be the product of an inhomogeneous wind of variable velocity. This is essentially a transmission model, and produces initially an absorption X-ray line spectrum, turning later into an emission spectrum, in which for Fe abundances 10 or 100 times solar the Fe line luminosities are $\lesssim 10^{42} - 10^{43}$ erg s^{-1}. The other model assumes a funnel geometry and is essentially a reflection model, with an empty or low density region along an axis, such as would arise in a rotating stellar envelope or a wind. The fireball and the afterglow propagate inside this funnel, which acts as a channel that collimates and reflects the continuum. This results in an emission line spectrum (Fig. 2), where for 10 or 100 times solar abundances the Fe K-α line luminosity reaches $L_{Fe} \lesssim 10^{44}$ erg s^{-1}, with line and edge equivalent widths $EW \lesssim 1$ keV. This is comparable to the 3σ Fe features reported by two groups [21,22] in GRB 970508 and GRB 970828.

It is interesting that the Fe K-edge is significant in a funnel model such as shown in Figure 2. While the energy of an Fe line 6.7 keV feature in GRB 970508 agrees with its previously known redshift $z = 0.835$, the line feature of GRB 970828 would be in agreement with the 9.28 keV Fe K-edge energy at this object's newly reported

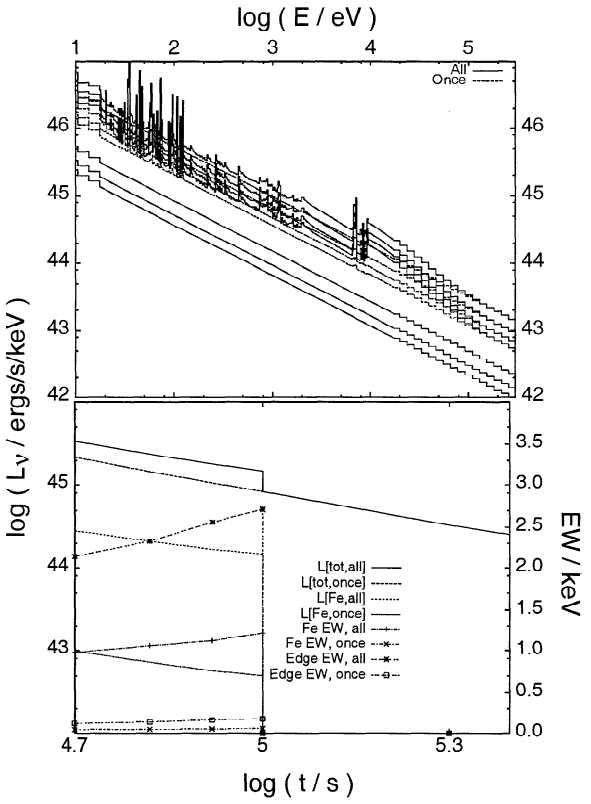

FIGURE 2. Model hypernova funnel spectrum (top) for observer times of 50, 66, 83, 100, 200, 300 ks top to bottom, and (bottom) the total and Fe light curves and equivalent widths [20], for $R = 1.5 \times 10^{16}$ cm, $n = 10^{10}$ cm^{-3}, and Fe abundance 10^2 times solar.

[23] redshift of $z = 0.958$. The line features in the 30–40 eV source-frame range seen in Figure 2 would be redshifted into the optical for $z \gtrsim 5$, but are likely to be blanketed by the Ly-α forest of intervening high-redshift galaxies. However, it may be possible to detect the soft X-ray metallic lines which become prominent soon after the Fe features, as the continuum softens and the gas cools, e.g., S and Si in the 2–3 keV source-frame range, or ~1–1.5 keV at $z \sim 1$.

ACKNOWLEDGMENTS

I am grateful to M.J. Rees, C. Weth and T. Kallman for stimulating collaborations, NASA NAG-5 2857, the Guggenheim Foundation and the Division of Physics, Math & Astronomy, the Astronomy Visitor and the Merle Kingsley funds at Caltech for support.

REFERENCES

1. Preece, R., et al., *ApJ* **496**, 849 (1998).

2. Crider, A., et al., *ApJ* **479**, L39 (1997).
3. Liang, E., et al., *ApJ* **491**, L15 (1997).
4. Liang, E., et al., *ApJ* **519**, L21 (1999).
5. Brainerd, J., et al., in *Abstr 19th Texas Symp*, Paris, astro-ph/9904039 (1999).
6. Dermer, C.D., et al., *ApJ* **515**, L49 (1999).
7. Brainerd, J., et al., *ApJ* **501**, 325 (1998).
8. Eichler, D. & Levinson, A., *ApJ*, submitted, astro-ph/9903103 (1999).
9. Thompson, C., *MNRAS* **270**, 480 (1994).
10. Mészáros , P. & Rees, M.J., *ApJ*, in press, astro-ph/9908126 (1999).
11. Mészáros , P., Laguna, P. & Rees, M.J., *ApJ* **415**, 181 (1993).
12. Rees, M.J. & Mészáros , P., *ApJ* **430**, L93 (1994).
13. Ghisellini, G. and Celotti, A., *ApJ* **511**, L93 (1999).
14. Bisnovatyi-Kogan, G. & Timokhin, A., *Astr. Rep.* **41**, 423 (1997).
15. Perna, R. & Loeb, A., *ApJ* **503**, L135 (1998).
16. Mészáros , P. & Rees, M.J., *MNRAS* **299**, L10 (1998).
17. Mészáros , P. & Rees, M.J., *ApJ* **502**, L105 (1998).
18. Ghisellini, G., et al., astro-ph/9808156 (1998).
19. Böttcher, M., et al., astro-ph/9809156 (1998).
20. Weth, C., Mészáros , P., Kallman, T. & Rees, M.J, *ApJ*, submitted, astro-ph/9908243 (1999).
21. Piro, L., et al., in *Proc. Rome GRB Conference*, *A&AS*, in press (1999).
22. Yoshida, A., et al., in *Proc. Rome GRB Conference*, *A&AS*, in press (1999).
23. Djorgovski, S.G., et al., *ApJ*, submitted (2000).